Structural Engineering and Mechanics, *Vol. 66, No. 2 (2018) 249-262*
DOI: https://doi.org/10.12989/sem.2018.66.2.249

Three dimensional dynamic response of functionally graded nanoplates under a moving load

Shahrokh Hosseini-Hashemi*[1,2] and Hossein Bakhshi Khaniki[1a]

[1]*School of Mechanical Engineering, Iran University of Science and Technology, Narmak, 16846-13114, Tehran, Iran*
[2]*Center of Excellence in Railway Transportation, Iran University of Science and Technology, Narmak, 16842-13114, Tehran, Iran*

(Received October 12, 2017, Revised February 3, 2018, Accepted February 7, 2018)

Abstract. In this paper, reaction of functionally graded (FG) thick nanoplates resting on a viscoelastic foundation to a moving nanoparticle/load is investigated. Nanoplate is assumed to be thick by using second order shear deformation theory and small-scale effects are taken into account in the framework of Eringen's nonlocal theory. Material properties are varied through the thickness using FG models by having power-law, sigmoid and exponential functions for material changes. FG nanoplate is assumed to be on a viscoelastic medium which is modeled using Kelvin-Voight viscoelastic model. Galerkin, state space and fourth-order Runge-Kutta methods are employed to solve the governing equations. A comprehensive parametric study is presetned to show the influence of different parameters on mechanical behavior of the system. It is shown that material variation in conjunction with nonlocal term have a significant effect on the dynamic deformation of nanoplate which could be used in comprehending and designing more efficient nanostructures. Moreover, it is shown that having a viscoelastic medium could play an important role in decreasing these dynamic deformations. With respect to the fresh studies on moving atoms, molecules, cells, nanocars, nanotrims and point loads on different nanosctructures using scanning tunneling microscopes (STM) and atomic force microscopes (AFM), this study could be a step forward in understanding, predicting and controlling such kind of behaviors by showing the influence of the moving path, velocity etc. on dynamic reaction of the plate.

Keywords: functionally graded material; forced deformation; FGM; nanoplate; second order shear deformation; moving load

1. Introduction

Nowadays composite materials are widely being used in different engineering subjects in both macro and small-scale structures. Functionally graded (FG) materials are a class of composites with the ability of gradual variation of some particular physical characteristics in at least one direction from a material to another which could be defined in a functional form. This practical property of FG materials led to using them in different systems such as diodes, sensors, heat conductors, electronic devices (El-Wazery and El-Desouky 2015), biomedical and orthopedic (Sola *et al.* 2016). Accordingly, in order to be able to design an efficient system using FG plates, it is necessary to fully understand the behavior of FG materials in different mechanical conditions. Many researchers studied the behavior of this class of composite materials in different mechanical conditions (Xiong and Tian 2017, Beldjelili *et al.* 2016, Bouderba *et al.* 2013, 2016, Bousahla *et al.* 2016, Akbaş 2017, Meftah *et al.* 2017, Hebali *et al.* 2016, Houari 2016, Uysal 2016, Sallai *et al.* 2015, Hashemi and Khaniki 2016a, Arefi 2015, Talha and Singh 2010, Chikh *et al.* 2017, Fahsi *et al.* 2017, Hamidi *et al.* 2015, Menasria *et al.* 2017, Tounsi *et al.* 2013, Zidi *et al.* 2014).

Moreover, by the improvements done in engineer designing, nanoplates and nanobeams became an important element in many systems with application in nanosensors, small magnetic memories, NEMS/MEMS devices, oscillators, Metamaterials etc. Nano-sized FG materials such as FG nanoplates benefits from both advantages of material property variation and the practical behavior of nanosize materials. Decreasing the dimensions into micro/nano scales changes the mechanical behavior in materials which could not be followed using classical continuum theories. Such kind of extraordinary behavior in nanoscale materials led to using nanosctructures in different fields of mechanical, chemical and electronic studies. Accordingly, to be able to describe and predict the behavior of nano/micro scale materials, different theories (Mindlin and Eshel 1968, Lomakin 1966, Eringen 2002) were presented in which the Eringen's differential nonlocal elastic theory is one of the most practical models among them all. In this non-classical continuum theory, it is assumed that stress at a point is a function of strains in all points in the continuum model depending on a nonlocal coefficient. Many researchers used non-classical elasticity theories to describe the behaviors of small-scale structures in static (Chaht *et al.* 2015, Rajaskaran and Khaniki 2017, Barati *et al.* 2016, Nguyen *et al.* 2017) and dynamic (Tahouneh 2017, Arani *et al.* 2017, Hashemi and Khaniki 2016b, Khaniki *et al.* 2017, Khaniki and Hashemi 2017a, b, c, d, Moradi-Dastjerdi and Momeni 2016, Bounouara *et al.* 2016, Khaniki 2018) conditions. Accordingly, nano-scale

*Corresponding author, Professor
E-mail: shh@iust.ac.ir
[a]Ph.D.
E-mail: h_bakhshi@mecheng.iust.ac.ir

ISSN: 1225-4568 (Print), 1598-6217 (Online)

structures were also analyzed in different conditions using nonlocal elastic theory (Bouafia *et al.* 2017, Bounouara *et al.* 2016, Besseghier *et al.* 2017, Zemri *et al.* 2015, Ahouel *et al.* 2016, Mouffoki *et al.* 2017, Belkorissat *et al.* 2015, Amar *et al.* 2017, Khetir *et al.* 2017, Chaht *et al.* 2015). One of the most appearing dynamic conditions in which small-scale plates and beams face with, is being under a moving load or mass. By being able to use scanning tunneling microscopes (STM) and atomic force microscopes (AFM) to move atoms, molecules, cells, nanocars, nanotrims, etc. on surfaces, it is essential to understand the behavior of the underneath structure. For the sake of understanding this type of mechanical behavior, some studies modeled the moving mass/load on small-scale structures. Kiani (2011a, b, 2013) investigated the reaction of nanoplates with respect to moving nanoparticle. Kirchhoff, Mindlin and higher order plate theories were used to model the nanoplate and the boundaries were assumed to be simply supported. Nanoparticle was assumed to move with a constant velocity on a linear and circular path. Using Laplace transform method, deformations were achieved for different nonlocal parameters and timelines. Bakhshi Khaniki and Hosseini-Hashemi (2017e) analyzed the dynamic response of double layered orthotropic thin plates under a moving nanoparticle. Each plate was assumed to be under an inplane load and the nanoparticle was assumed to move in linear and circular paths. Governing equations were solved using a conjunction of integral convolution and Laplace method. Shahsavari *et al.* (2017) investigated the mechanical reaction of single layered nanoplates under the moving concentrated load coupled by a visco-Pasternak foundation in a hygro-thermal environment. Shahsavari and Janghorban (2017) also studied the time-dependent bending and shearing responses of single layered nanoplates under a moving load. Nonlocal elasticity theory, two-variable refined plate theory and Hamilton's principle were used to reach the governing equations and solved by using state-space and Navier methods Ghorbanpour Arani *et al.* (2015) studied the dynamic response of an embedded poly-vinylidene fluoride (PVDF) nanoplates under a moving nanoparticle on an arbitrary elliptical path. It was assumed that nanoplate was on an elastic foundation and under biaxial loading. Nanoplate was modeled after Kirchhoff plate theory and the elastic medium was modeled by Pasternak foundation. Based on Eringen's nonlocal theory, energy method and Hamilton's principle, equations of motion were derived and by using Galerkin method the closed-form solutions were achieved. Nami and Janghorban (2015) studied the dynamic analysis of isotropic nanoplates subjected to moving load. The movement of load was assumed to be in a straight simple line on x axis with constant velocity. Second order shear deformation was used to reach the equations and it were solved using state space method. Effects of aspect ratio, nonlocal parameter and velocity parameter on maximum deflection of nanoplate were studied. Hosseini Hashemi and Bakhshi Khaniki (2017a, b) studied the dynamic behavior of multi-layered micro/nanobeam systems with respect to a moving nanoparticle. Coupling between layers were modeled by Winkler theory for elastic and Kelvin-Voigt theory for viscoelastic models and moreover, nanobeams were modeled by Euler-Bernoulli beam theory while nanoparticle was assumed to move in a straight line with constant velocity. Equations of motion were solved using Galerkin and Laplace transform methods. Analytical solutions were presented for low-layered systems and numerical results were achieved for high-layered ones. Also, effects of having a medium under the model was studied. Parametric study was presented to show the influence of the number of layers, viscoelastic coupling, nonlocal parameter etc. on dynamic deflection of each layer.

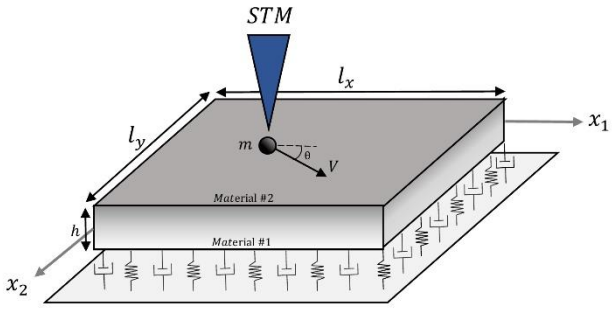

Fig. 1 Schematic representation of FG nanoplate resting on a viscoelastic foundation carrying a moving nanoparticle

To the best knowledge of the authors, there have been no studies done in order to comprehend the dynamic behavior of FG nanoplates with or without foundation under a moving load or nanoparticle. Previous studies on material varying structures have shown that using higher order shear deformation theories could lead to more accurate results (Abualnour *et al.* 2018, Meziane *et al.* 2014, Yahia *et al.* 2015, Belabed *et al.* 2014, Bellifa *et al.* 2016, Bennoun *et al.* 2016, Bourada *et al.* 2015, Draiche *et al.* 2016, Hebali *et al.* 2014, Mahi and Tounsi 2015, Saidi *et al.* 2016). In this study, by using second order shear deformation theory, dynamic response of different types of FG nanoplates resting on viscoelastic foundation is investigated while the nanoparticle/load passes through. An arbitrary linear path is used to model the nanoparticles movement and furthermore, a comprehensive parametric study is presented to fully understand the effects of different designing and natural parameters on dynamic behavior of the system. Accordingly, Fig. 1 shows a schematic representation of FG nanoplates resting on a viscoelastic medium with a nanoparticle moving on the top surface. Movement of this nanoparticle which could be an atom, molecule, nanocar, nanotrim or a concentrated force could be done using STM and AFM systems.

2. Problem formulations

By using second order shear deformation theory, displacement terms in each direction could be written as (Panyatong *et al.* 2016)

$$\begin{cases} u = u^0 + x_3\varphi_1 + x_3^2\varphi_2 \\ v = v^0 + x_3\psi_1 + x_3^2\psi_2 \\ w = w(x_1, x_2) \end{cases} \quad (1)$$

In which u^0 and v^0 are the inplane displacements of

middle plane in x_1 and x_2 directions, $\varphi_1.\varphi_2.\psi_1$ and $\psi_2$are the rotations of transverse normal to x_1 and x_2 axis and w describes the transverse deflection of nanoplate. Strain equations due to Eq. (1) could be presented a

$$\begin{cases}\varepsilon_{11}=\varepsilon_{11}^0+zK_{11}^0+z^2K_{11}^1\\ \quad=\dfrac{\partial u}{\partial x_1}+z\dfrac{\partial\varphi_1}{\partial x_1}+z^2\dfrac{\partial\varphi_2}{\partial x_1}\\ \varepsilon_{22}=\varepsilon_{22}^0+zK_{22}^0+z^2K_{22}^1\\ \quad=\dfrac{\partial v}{\partial x_2}+z\dfrac{\partial\psi_1}{\partial x_2}+z^2\dfrac{\partial\psi_2}{\partial x_2}\\ \gamma_{12}=\gamma_{12}^0+zK_{12}^0+z^2K_{12}^1\\ \quad=\dfrac{\partial u}{\partial x_2}+\dfrac{\partial v}{\partial x_1}+z\left(\dfrac{\partial\varphi_1}{\partial x_2}+\dfrac{\partial\psi_1}{\partial x_1}\right)+z^2\left(\dfrac{\partial\varphi_2}{\partial x_2}+\dfrac{\partial\psi_2}{\partial x_1}\right)\\ \gamma_{23}=\gamma_{23}^0+z\gamma_{23}^1=\psi_1+\dfrac{\partial w}{\partial x_2}+2z\psi_2\\ \gamma_{13}=\gamma_{13}^0+z\gamma_{13}^1=\varphi_1+\dfrac{\partial w}{\partial x_1}+2z\varphi_2\end{cases}\tag{2}$$

in which ε_{11}, ε_{22} are the normal strains in x_1 and x_2 directions and γ_{12}, γ_{13} and γ_{23} are the shear strain parameters. Equation of motion of plates with respect to second order shear deformation theory is given as

$$\begin{cases}\dfrac{\partial N_{x_1}}{\partial x_1}+\dfrac{\partial N_{x_1x_2}}{\partial x_2}=I_1\ddot{u}+I_2\ddot{\varphi}_1+I_3\ddot{\varphi}_2\\ \dfrac{\partial N_{x_2}}{\partial x_2}+\dfrac{\partial N_{x_1x_2}}{\partial x_1}=I_1\ddot{v}+I_2\ddot{\psi}_1+I_3\ddot{\psi}_2\\ \dfrac{\partial Q_{x_1}}{\partial x_1}+\dfrac{\partial Q_{x_2}}{\partial x_2}+q=I_1\ddot{w}\\ \dfrac{\partial M_{x_1}}{\partial x_1}+\dfrac{\partial M_{x_1x_2}}{\partial x_2}-Q_{xz}=I_2\ddot{u}+I_3\ddot{\varphi}_1+I_4\ddot{\varphi}_2\\ \dfrac{\partial M_{x_2}}{\partial x_2}+\dfrac{\partial M_{x_1x_2}}{\partial x_1}-Q_{yz}=I_2\ddot{v}+I_3\ddot{\psi}_1+I_4\ddot{\psi}_2\\ \dfrac{\partial L_{x_1}}{\partial x_1}+\dfrac{\partial L_{x_1x_2}}{\partial x_2}-2R_{xz}=I_3\ddot{u}+I_4\ddot{\varphi}_1+I_5\ddot{\varphi}_2\\ \dfrac{\partial L_{x_2}}{\partial x_2}+\dfrac{\partial L_{x_1x_2}}{\partial x_1}-2R_{yz}=I_3\ddot{v}+I_4\ddot{\psi}_1+I_5\ddot{\psi}_2\end{cases}\tag{3}$$

where q is the applied external force due to the moving load/nanoparticles and the reaction of viscoelastic medium, I_1 to I_5 are the mass inertia factors and N_i, M_i, L_i, Q_i and R_i are the stress resultants defined as

(4)

where σ is the stress parameter. In order to add the nonlocal effects of nanoscale plates, Eringen's nonlocal theory is presented as (Eringen 2002)

$$\left(1-\mu\nabla^2\right)\sigma=C_{ijkl}\varepsilon\tag{5}$$

in which C_{ijkl} is the fourth-order elasticity tensor, μ is the material constant which is defined as (e_0a_0/l) where a_0 and l are internal and external characteristic size and e_0 is a constant number depending on the material. Furthermore, by using the principle of virtual displacements and Eq. (2) to Eq. (5), equations of motion of the nonlocal second order shear deformation theory will be derived as

$$\begin{aligned}&\left(1-\mu\nabla^2\right)\left(I_1\ddot{u}+I_2\ddot{\varphi}_1+I_3\ddot{\varphi}_2\right)=\\ &\left[A_{11}\frac{\partial^2u}{\partial x_1^{\,2}}+A_{66}\frac{\partial^2u}{\partial x_2^{\,2}}+\left(A_{12}+A_{66}\right)\frac{\partial^2v}{\partial x_1\partial x_2}\right]\\ &+\left[B_{11}\frac{\partial^2\varphi_1}{\partial x_1^{\,2}}+B_{66}\frac{\partial^2\varphi_1}{\partial x_2^{\,2}}\right]+\left[D_{11}\frac{\partial^2\varphi_2}{\partial x_1^{\,2}}+D_{66}\frac{\partial^2\varphi_2}{\partial x_2^{\,2}}\right]\\ &+\left[B_{12}\frac{\partial^2\psi_1}{\partial x_1\partial x_2}+B_{66}\frac{\partial^2\psi_1}{\partial x_1\partial x_2}\right]+\left[D_{12}\frac{\partial^2\psi_2}{\partial x_1\partial x_2}+D_{66}\frac{\partial^2\psi_1}{\partial x_1\partial x_2}\right]\end{aligned}\tag{6}$$

$$\begin{aligned}&\left(1-\mu\nabla^2\right)\left(I_1\ddot{v}+I_2\ddot{\psi}_1+I_3\ddot{\psi}_2\right)=\\ &\left[A_{22}\frac{\partial^2v}{\partial x_2^{\,2}}+A_{66}\frac{\partial^2v}{\partial x_1^{\,2}}+\left(A_{12}+A_{66}\right)\frac{\partial^2u}{\partial x_1\partial x_2}\right]\\ &+\left[B_{22}\frac{\partial^2\psi_1}{\partial x_2^{\,2}}+B_{66}\frac{\partial^2\psi_1}{\partial x_1^{\,2}}\right]+\left[D_{22}\frac{\partial^2\psi_2}{\partial x_2^{\,2}}+D_{66}\frac{\partial^2\psi_2}{\partial x_1^{\,2}}\right]\\ &+\left[B_{12}\frac{\partial^2\varphi_1}{\partial x_1\partial x_2}+B_{66}\frac{\partial^2\varphi_1}{\partial x_1\partial x_2}\right]+\left[D_{12}\frac{\partial^2\varphi_2}{\partial x_1\partial x_2}+D_{66}\frac{\partial^2\varphi_2}{\partial x_1\partial x_2}\right]\end{aligned}\tag{7}$$

$$\begin{aligned}&\left(1-\mu\nabla^2\right)\left(I_1\ddot{w}-q\right)=\\ &\left[A_{55}\frac{\partial^2w}{\partial x_1^{\,2}}+A_{44}\frac{\partial^2w}{\partial x_2^{\,2}}\right]+\left[A_{55}\frac{\partial\varphi_1}{\partial x_1}\right]\\ &+\left[2B_{55}\frac{\partial\varphi_2}{\partial x_1}\right]+\left[A_{44}\frac{\partial\psi_1}{\partial x_2}\right]+\left[2B_{44}\frac{\partial\psi_2}{\partial x_1}\right]\end{aligned}\tag{8}$$

$$\begin{aligned}&\left(1-\mu\nabla^2\right)\left(I_2\ddot{u}+I_3\ddot{\varphi}_1+I_4\ddot{\varphi}_2\right)=\\ &\left[B_{11}\frac{\partial^2u}{\partial x_1^{\,2}}+B_{66}\frac{\partial^2u}{\partial x_2^{\,2}}+\left(B_{12}+B_{66}\right)\frac{\partial^2v}{\partial x_1\partial x_2}\right]\\ &+\left[D_{11}\frac{\partial^2\varphi_1}{\partial x_1^{\,2}}+D_{66}\frac{\partial^2\varphi_1}{\partial x_2^{\,2}}\right]+\left[E_{11}\frac{\partial^2\varphi_2}{\partial x_1^{\,2}}+E_{66}\frac{\partial^2\varphi_2}{\partial x_2^{\,2}}\right]\\ &-A_{55}\left(\varphi_1+\frac{\partial w}{\partial x_1}\right)+\left[D_{12}\frac{\partial^2\psi_1}{\partial x_1\partial x_2}+D_{66}\frac{\partial^2\psi_1}{\partial x_1\partial x_2}\right]\\ &+\left[E_{12}\frac{\partial^2\psi_2}{\partial x_1\partial x_2}+E_{66}\frac{\partial^2\psi_1}{\partial x_1\partial x_2}\right]-B_{55}\left(2\varphi_2\right)\end{aligned}\tag{10}$$

$$\begin{aligned}&\left(1-\mu\nabla^2\right)\left(I_3\ddot{u}+I_4\ddot{\varphi}_1+I_5\ddot{\varphi}_2\right)=\\ &\left[D_{11}\frac{\partial^2u}{\partial x_1^{\,2}}+D_{66}\frac{\partial^2u}{\partial x_2^{\,2}}+\left(D_{12}+D_{66}\right)\frac{\partial^2v}{\partial x_1\partial x_2}\right]\\ &+\left[E_{11}\frac{\partial^2\varphi_1}{\partial x_1^{\,2}}+E_{66}\frac{\partial^2\varphi_1}{\partial x_2^{\,2}}\right]+\left[F_{11}\frac{\partial^2\varphi_2}{\partial x_1^{\,2}}+F_{66}\frac{\partial^2\varphi_2}{\partial x_2^{\,2}}\right]\\ &-2B_{55}\left(\varphi_1+\frac{\partial w}{\partial x_1}\right)+\left[E_{12}\frac{\partial^2\psi_1}{\partial x_1\partial x_2}+E_{66}\frac{\partial^2\psi_1}{\partial x_1\partial x_2}\right]\\ &+\left[F_{12}\frac{\partial^2\psi_2}{\partial x_1\partial x_2}+F_{66}\frac{\partial^2\psi_1}{\partial x_1\partial x_2}\right]-2D_{55}\left(2\varphi_2\right)\end{aligned}\tag{11}$$

$$\begin{aligned}&\left(1-\mu\nabla^2\right)\left(I_3\ddot{v}+I_4\ddot{\psi}_1+I_5\ddot{\psi}_2\right)=\\ &\left[D_{22}\frac{\partial^2v}{\partial x_2^{\,2}}+D_{66}\frac{\partial^2v}{\partial x_1^{\,2}}+\left(D_{12}+D_{66}\right)\frac{\partial^2u}{\partial x_1\partial x_2}\right]\\ &+\left[E_{22}\frac{\partial^2\psi_1}{\partial x_2^{\,2}}+E_{66}\frac{\partial^2\psi_1}{\partial x_1^{\,2}}\right]+\left[F_{22}\frac{\partial^2\psi_2}{\partial x_2^{\,2}}+F_{66}\frac{\partial^2\psi_2}{\partial x_1^{\,2}}\right]\\ &-2B_{44}\left(\psi_1+\frac{\partial w}{\partial x_2}\right)+\left[E_{12}\frac{\partial^2\varphi_1}{\partial x_1\partial x_2}+E_{66}\frac{\partial^2\varphi_1}{\partial x_1\partial x_2}\right]\\ &+\left[F_{12}\frac{\partial^2\varphi_2}{\partial x_1\partial x_2}+F_{66}\frac{\partial^2\varphi_2}{\partial x_1\partial x_2}\right]-2D_{44}\left(2\psi_2\right)\end{aligned}\tag{12}$$

where A_{ii}, B_{ii}, D_{ii}, D_{ii} and E_{ii} are the material constants defined as

$$\begin{cases} I_i = \int_{-\frac{h}{2}}^{\frac{h}{2}} \rho x_3^{i-1} dx_3, \quad i = 1,2,\ldots,5 \\ \{N_i, M_i, L_i\} = \int_{-\frac{h}{2}}^{\frac{h}{2}} \sigma_i \{1, x_3, x_3^2\} dx_3, \quad i = x_1, x_2, x_1x_2 \\ \{Q_i, R_i\} = \int_{-\frac{h}{2}}^{\frac{h}{2}} \sigma_i \{1, x_3, x_3^2\} dx_3, \quad i = x_1x_3, x_2x_3 \end{cases} \tag{13}$$

Material parameters are computed with respect to the material variation function. In this study, three kinds of FG materials will be discussed which includes sigmoid, exponential and power law material variation types and accordingly, the material parameters are computed for each model separately.

2.1 Sigmoid material variation model

Material properties for sigmoid FG materials are assumed to be as

$$\begin{cases} E(x_3) = (E_t - E_b)\left[\frac{1}{2}\left(\frac{h+2x_3}{h}\right)^S\right] + E_b & -\frac{h}{2} \le x_3 \le 0 \\ E(x_3) = (E_t - E_b)\left[1 - \frac{1}{2}\left(\frac{h-2x_3}{h}\right)^S\right] + E_b & 0 \le x_3 \le \frac{h}{2} \end{cases} \tag{14}$$

$$\begin{cases} \rho(x_3) = (\rho_t - \rho_b)\left[\frac{1}{2}\left(\frac{h+2x_3}{h}\right)^S\right] + \rho_b & -\frac{h}{2} \le x_3 \le 0 \\ \rho(x_3) = (\rho_t - \rho_b)\left[1 - \frac{1}{2}\left(\frac{h-2x_3}{h}\right)^S\right] + \rho_b & 0 \le x_3 \le \frac{h}{2} \end{cases} \tag{15}$$

where E and ρ are Young's modulus and density terms of materials. Using Eq. (16) and Eq. (17), $A_{11}$to E_{33} will be calculated as

$$A_{11} = \frac{h(E_t + E_b)}{2(1-\vartheta^2)}, \quad A_{12} = \vartheta A_{11}, \quad A_{22} = A_{11}, \quad A_{33} = \frac{h(G_t + G_b)}{2} \tag{16}$$

$$B_{11} = \frac{h^2 S(E_b - E_t)(S+3)}{8(1-\vartheta^2)(S^2+3S+2)}, \quad B_{12} = \vartheta B_{11}, \quad B_{22} = B_{11}, \quad B_{33} = \frac{h^2 p(G_b - G_t)(S+3)}{8(S^2+3S+2)} \tag{17}$$

$$C_{11} = \frac{h^3(E_t + E_b)}{24(1-\vartheta^2)}, \quad C_{12} = \vartheta C_{11}, \quad C_{22} = C_{11}, \quad C_{33} = \frac{h^3(G_t + G_b)}{24} \tag{18}$$

$$D_{11} = \frac{h^4 S(S+5)(S^2+5S+10)(E_b - E_t)}{64(1-\vartheta^2)(S^4+10S^3+35S^2+50S+24)}, \quad D_{12} = \vartheta D_{11}, \quad D_{22} = D_{11}, \quad D_{33} = \frac{h^4 S(S+5)(S^2+5S+10)(G_b - G_t)}{64(S^4+10S^3+35S^2+50S+24)} \tag{19}$$

$$E_{11} = \frac{h^5(E_b + E_t)}{(1-\vartheta^2)160}, \quad E_{12} = \vartheta E_{11}, \quad E_{22} = E_{11}, \quad E_{33} = \frac{h^5(G_b + G_t)}{160} \tag{20}$$

In which S is the sigmoid index term and I_i will be achieved as

$$\begin{cases} I_1 = \frac{h(\rho_t + \rho_b)}{2} \\ I_2 = \frac{-h^2 S(\rho_b - \rho_t)(S+3)}{8(S^2+3S+2)} \\ I_3 = \frac{h^3(\rho_t + \rho_b)}{24} \\ I_4 = \frac{-h^4 S(S+5)(S^2+5S+10)(\rho_b - \rho_t)}{64(S^4+10S^3+35S^2+50S+24)} \\ I_5 = \frac{h^5(\rho_t + \rho_b)}{160} \end{cases} \tag{21}$$

2.2 Exponential material variation model

In the same way, material properties for exponential FG materials are

$$\begin{cases} E(x_3) = E_b e^{\varnothing x_3} \\ \rho(x_3) = \rho_b e^{\varnothing x_3} \end{cases} \tag{22}$$

in which $\emptyset$ is the exponential model index and the material parameters $A_{11}$to E_{33} are presented as

$$A_{11} = \frac{E_b\left(e^{\varnothing\frac{h}{2}} - e^{-\varnothing\frac{h}{2}}\right)}{\varnothing(1-\vartheta^2)}, \quad A_{12} = \vartheta A_{11}, \quad A_{22} = A_{11}, \quad A_{33} = \frac{G_b\left(e^{\varnothing\frac{h}{2}} - e^{-\varnothing\frac{h}{2}}\right)}{\varnothing} \tag{23}$$

$$B_{11} = \frac{E_b\left((h\varnothing-2)e^{\varnothing\frac{h}{2}} + (h\varnothing+2)e^{-\varnothing\frac{h}{2}}\right)}{2\varnothing^2(1-\vartheta^2)}, \quad B_{12} = \vartheta B_{11}, \quad B_{22} = B_{11}, \quad B_{33} = \frac{G_b\left((h\varnothing-2)e^{\varnothing\frac{h}{2}} + (h\varnothing+2)e^{-\varnothing\frac{h}{2}}\right)}{2\varnothing^2(1-\vartheta^2)} \tag{24}$$

$$C_{11} = \frac{E_b\left((h^2\varnothing^2 - 4h\varnothing + 8)e^{\varnothing\frac{h}{2}} - (h^2\varnothing^2 + 4h\varnothing + 8)e^{-\varnothing\frac{h}{2}}\right)}{4\varnothing^3(1-\vartheta^2)}, \quad C_{12} = \vartheta C_{11}, \quad C_{22} = C_{11}, \quad C_{33} = \frac{G_b\left((h^2\varnothing^2 - 4h\varnothing + 8)e^{\varnothing\frac{h}{2}} - (h^2\varnothing^2 + 4h\varnothing + 8)e^{-\varnothing\frac{h}{2}}\right)}{4\varnothing^3} \tag{25}$$

$$D_{11} = \frac{E_b\left((h^3\varnothing^3 - 6h^2\varnothing^2 + 24h\varnothing - 48)e^{\varnothing\frac{h}{2}}\right)}{8\varnothing^4(1-\vartheta^2)} + \frac{E_b\left((h^3\varnothing^3 + 6h^2\varnothing^2 + 24h\varnothing + 48)e^{-\varnothing\frac{h}{2}}\right)}{8\varnothing^4(1-\vartheta^2)}, \quad D_{12} = \vartheta D_{11}, \quad D_{22} = D_{11}, \quad D_{33} = \frac{G_b\left((h^3\varnothing^3 - 6h^2\varnothing^2 + 24h\varnothing - 48)e^{\varnothing\frac{h}{2}}\right)}{8\varnothing^4} + \frac{G_b\left((h^3\varnothing^3 + 6h^2\varnothing^2 + 24h\varnothing + 48)e^{-\varnothing\frac{h}{2}}\right)}{8\varnothing^4} \tag{26}$$

$$
\begin{aligned}
E_{11} &= \frac{E_b\left(\left(h^4\varnothing^4-8h^3\varnothing^3+48h^2\varnothing^2-192h\varnothing+384\right)e^{\varnothing\frac{h}{2}}\right)}{16\varnothing^5\left(1-\vartheta^2\right)} \\
&- \frac{E_b\left(\left(h^4\varnothing^4+8h^3\varnothing^3+48h^2\varnothing^2+192h\varnothing+384\right)e^{-\varnothing\frac{h}{2}}\right)}{16\varnothing^5\left(1-\vartheta^2\right)}, \\
E_{12} &= \vartheta E_{11}, \quad E_{22} = E_{11}, \\
E_{33} &= \frac{G_b\left(\left(h^4\varnothing^4-8h^3\varnothing^3+48h^2\varnothing^2-192h\varnothing+384\right)e^{\varnothing\frac{h}{2}}\right)}{16\varnothing^5\left(1-\vartheta^2\right)} \\
&- \frac{G_b\left(\left(h^4\varnothing^4+8h^3\varnothing^3+48h^2\varnothing^2+192h\varnothing+384\right)e^{-\varnothing\frac{h}{2}}\right)}{16\varnothing^5\left(1-\vartheta^2\right)}
\end{aligned} \tag{27}
$$

and the mass inertia parameters are

$$
\begin{cases}
I_1 = \dfrac{\rho_b\left(e^{\varnothing\frac{h}{2}}-e^{-\varnothing\frac{h}{2}}\right)}{\varnothing} \\
I_2 = \dfrac{\rho_b\left((h\varnothing-2)e^{\varnothing\frac{h}{2}}+(h\varnothing+2)e^{-\varnothing\frac{h}{2}}\right)}{2\varnothing^2} \\
I_3 = \dfrac{\rho_b\left(\left(h^2\varnothing^2-4h\varnothing+8\right)e^{\varnothing\frac{h}{2}}-\left(h^2\varnothing^2+4h\varnothing+8\right)e^{-\varnothing\frac{h}{2}}\right)}{4\varnothing^3} \\
I_4 = \dfrac{\rho_b\left(\left(h^3\varnothing^3-6h^2\varnothing^2+24h\varnothing-48\right)e^{\varnothing\frac{h}{2}}\right)}{8\varnothing^4} \\
\quad + \dfrac{\rho_b\left(\left(h^3\varnothing^3+6h^2\varnothing^2+24h\varnothing+48\right)e^{-\varnothing\frac{h}{2}}\right)}{8\varnothing^4} \\
I_5 = \dfrac{\rho_b\left(\left(h^4\varnothing^4-8h^3\varnothing^3+48h^2\varnothing^2-192h\varnothing+384\right)e^{\varnothing\frac{h}{2}}\right)}{16\varnothing^5} \\
\quad - \dfrac{\rho_b\left(\left(h^4\varnothing^4+8h^3\varnothing^3+48h^2\varnothing^2+192h\varnothing+384\right)e^{-\varnothing\frac{h}{2}}\right)}{16\varnothing^5}
\end{cases} \tag{28}
$$

2.3 Power law material variation model

For power law functionally graded nanoplates, material properties are

$$
\begin{cases}
E\left(x_3\right) = \left(E_b - E_t\right)\left(\dfrac{h-2x_3}{2h}\right)^p + E_t \\
\rho\left(x_3\right) = \left(\rho_b - \rho_t\right)\left(\dfrac{h-2x_3}{2h}\right)^p + \rho_{ts}
\end{cases} \quad -\frac{h}{2} \le x_3 \le \frac{h}{2} \tag{29}
$$

where P is the power-law model index and the parameters A_{11} to E_{33} are calculated as

$$
\begin{aligned}
A_{11} &= \frac{h\left(E_t + E_b P\right)}{\left(1-\vartheta^2\right)\left(P+1\right)}, \quad A_{12} = \vartheta A_{11}, \\
A_{22} &= A_{11}, \quad A_{33} = \frac{h\left(G_t + G_b P\right)}{\left(P+1\right)}
\end{aligned} \tag{30}
$$

$$
\begin{aligned}
B_{11} &= \frac{h^2 P\left(E_b - E_t\right)}{\left(1-\vartheta^2\right)\left(2P^2+6P+4\right)}, \quad B_{12} = \vartheta B_{11}, \\
B_{22} &= B_{11}, \quad B_{33} = \frac{h^2 P\left(G_b - G_t\right)}{\left(2P^2+6P+4\right)}
\end{aligned} \tag{31}
$$

$$
\begin{aligned}
C_{11} &= \frac{h^3 P\left(E_b P^3 + 3\left(E_t + E_b\right)P^2 + \left(8E_b + 3E_1\right)P + 6E_t\right)}{12\left(1-\vartheta^2\right)\left(P^3+6P^2+11P+6\right)}, \\
C_{12} &= \vartheta C_{11}, \quad C_{22} = C_{11}, \\
C_{33} &= \frac{h^3 P\left(G_b P^3 + 3\left(G_t + G_b\right)P^2 + \left(8G_b + 3G_1\right)P + 6G_t\right)}{12\left(P^3+6P^2+11P+6\right)}
\end{aligned} \tag{32}
$$

$$
\begin{aligned}
D_{11} &= \frac{h^4 P\left(P^2+3P+8\right)\left(E_b - E_t\right)}{8\left(1-\vartheta^2\right)\left(P^4+10P^3+35P^2+50P+24\right)}, \\
D_{12} &= \vartheta D_{11}, \quad D_{22} = D_{11}, \\
D_{33} &= \frac{h^4 P\left(P^2+3P+8\right)\left(G_b - G_t\right)}{8\left(P^4+10P^3+35P^2+50P+24\right)}
\end{aligned} \tag{33}
$$

$$
\begin{aligned}
E_{11} &= \frac{h^5\left(E_b P^5 + 5\left(2E_b + E_t\right)P^4 + 5\left(11E_b + 6E_t\right)P^3\right)}{80\left(1-\vartheta^2\right)\left(P^5+15P^4+85P^3+225P^2+274P+120\right)} \\
&+ \frac{h^5\left(5\left(22E_b + 23E_t\right)P^2 + 2\left(94E_b + 45E_t\right)P + 120E_t\right)}{80\left(1-\vartheta^2\right)\left(P^5+15P^4+85P^3+225P^2+274P+120\right)} \\
E_{12} &= \vartheta E_{11}, \quad E_{22} = E_{11}, \\
E_{33} &= \frac{h^5\left(G_b P^5 + 5\left(2G_b + G_t\right)P^4 + 5\left(11G_b + 6G_t\right)P^3\right)}{80\left(P^5+15P^4+85P^3+225P^2+274P+120\right)} \\
&+ \frac{h^5\left(5\left(22G_b + 23G_t\right)P^2 + 2\left(94G_b + 45G_t\right)P + 120G_t\right)}{80\left(P^5+15P^4+85P^3+225P^2+274P+120\right)}
\end{aligned} \tag{34}
$$

and I_i will be achieved as

$$
\begin{cases}
I_1 = \dfrac{h\left(\rho_t + \rho_b P\right)}{\left(P+1\right)} \\
I_2 = \dfrac{h^2 P\left(\rho_b - \rho_t\right)}{2\left(P^2+3P+2\right)} \\
I_3 = \dfrac{h^3\left(\rho_b P^3 + 3\left(\rho_t + \rho_b\right)P^2 + \left(8\rho_b + 3\rho_t\right)P + 6\rho_t\right)}{12\left(p^3+6p^2+11p+6\right)} \\
I_4 = \dfrac{h^4 P\left(P^2+3P+8\right)\left(\rho_b - \rho_t\right)}{80\left(P^5+15P^4+85P^3+225P^2+274P+120\right)} \\
I_5 = \dfrac{h^5\left(\rho_b P^5 + 5\left(2\rho_b + \rho_t\right)P^4 + 5\left(11\rho_b + 6\rho_t\right)P^3\right)}{80\left(1-\vartheta^2\right)\left(P^5+15P^4+85P^3+225P^2+274P+120\right)} \\
\quad + \dfrac{h^5\left(5\left(22\rho_b + 23\rho_t\right)P^2 + 2\left(94\rho_b + 45\rho_t\right)P + 120\rho_t\right)}{80\left(1-\vartheta^2\right)\left(P^5+15P^4+85P^3+225P^2+274P+120\right)}
\end{cases} \tag{35}
$$

3. Solution procedure

By using Galerkin's method, deflections in nanoplate could be defined in mode shapes and accordingly, by having simply supported boundary condition for all edges, transverse deflections are expressed as

$$
\begin{cases}
u(x_1,x_2,t) = \sum_{j=1}^{m_j}\sum_{i=1}^{n_i} U_{ij}(t)\cos\left(\alpha x_1\right)\sin\left(\beta x_2\right) \\
v(x_1,x_2,t) = \sum_{j=1}^{m_j}\sum_{i=1}^{n_i} V_{ij}(t)\sin\left(\alpha x_1\right)\cos\left(\beta x_2\right) \\
w(x_1,x_2,t) = \sum_{j=1}^{m_j}\sum_{i=1}^{n_i} W_{ij}(t)\sin\left(\alpha x_1\right)\sin\left(\beta x_2\right) \\
\varphi_1(x_1,x_2,t) = \sum_{j=1}^{m_j}\sum_{i=1}^{n_i} \Phi_{ij1}(t)\cos\left(\alpha x_1\right)\sin\left(\beta x_2\right) \\
\psi_1(x_1,x_2,t) = \sum_{j=1}^{m_j}\sum_{i=1}^{n_i} \Psi_{ij1}(t)\sin\left(\alpha x_1\right)\cos\left(\beta x_2\right) \\
\varphi_2(x_1,x_2,t) = \sum_{j=1}^{m_j}\sum_{i=1}^{n_i} \Phi_{ij2}(t)\cos\left(\alpha x_1\right)\sin\left(\beta x_2\right) \\
\psi_2(x_1,x_2,t) = \sum_{j=1}^{m_j}\sum_{i=1}^{n_i} \Psi_{ij2}(t)\sin\left(\alpha x_1\right)\cos\left(\beta x_2\right)
\end{cases} \tag{36}
$$

where U, V, W, Φ_i, Ψ_i are the deflection parameters which only depends on the time variable t and n_i and m_j are the number of terms used to model the expansion series in which in this study for having a higher accuracy it is assumed to be 30. The external force applied on the plate is written as $q = q_p - q_w$ where q_p is the applied force due to the moving nanoparticle while q_w is the viscoelastic medium reaction force which could be defined using Dirac terms in series form as

$$\begin{aligned} &q_p = m_p g\delta(x_1 - x_p)\delta(x_2 - y_p) = \\ &\frac{4m_p g}{L_x L_y}\sum_{j=1}^{m_j}\sum_{i=1}^{n_i}\sin(\alpha x_p)\sin(\alpha x_1)\sin(\beta y_p)\sin(\beta x_2) \\ &q_w = K_W w(x_1,x_2,t) + C_w \dot{w}(x_1,x_2,t) = \\ &\sum_{j=1}^{m_j}\sum_{i=1}^{n_i} K_W W(t)\sin(\alpha x_1)\sin(\beta x_2) + C_w \dot{W}(t)\sin(\alpha x_1)\sin(\beta x_2) \end{aligned} \tag{37}$$

in which m_p, x_p and y_p are the mass and instance position of nanoparticle, L_x and L_y are the length of the nanoplate in x_1 and x_2 directions and K_W and C_W are the stiffness and damping parameters of Kelvin-Voigt viscoelastic foundation. By having mass inertia and material constants for different type of FG nanoplates, Eq. (6) to Eq. (12) could be written in matrix form by using Eq. (36) and Eq. (37) as

$$[\lambda_{ij}]\begin{Bmatrix}\ddot{U}\\ \ddot{V}\\ \ddot{W}\\ \ddot{\Phi}_1\\ \ddot{\Psi}_1\\ \ddot{\Phi}_2\\ \ddot{\Psi}_2\end{Bmatrix} + [\zeta_{ij}]\begin{Bmatrix}\dot{U}\\ \dot{V}\\ \dot{W}\\ \dot{\Phi}_1\\ \dot{\Psi}_1\\ \dot{\Phi}_2\\ \dot{\Psi}_2\end{Bmatrix} + [\kappa_{ij}]\begin{Bmatrix}U\\ V\\ W\\ \Phi_1\\ \Psi_1\\ \Phi_2\\ \Psi_2\end{Bmatrix} = \{F_{ij}\} \tag{38}$$

in which $[\lambda_{ij}]$, $[\xi_{ij}]$ and $[\kappa_{ij}]$ are the coefficient matrices and $\{F_{ij}\}$ is the force vector defined as

$$\lambda_{ij} = (1+\mu(\alpha^2+\beta^2))\begin{bmatrix} I_1 & 0 & 0 & I_2 & 0 & I_3 & 0\\ 0 & I_1 & 0 & 0 & I_2 & 0 & I_3\\ 0 & 0 & I_1 & 0 & 0 & 0 & 0\\ I_2 & 0 & 0 & I_3 & 0 & I_4 & 0\\ 0 & I_2 & 0 & 0 & I_3 & 0 & I_4\\ I_3 & 0 & 0 & I_4 & 0 & I_5 & 0\\ 0 & I_3 & 0 & 0 & I_4 & 0 & I_5 \end{bmatrix} \tag{39}$$

$$\zeta_{ij} = \begin{bmatrix} 0 & 0 & 0 & 0 & 0 & 0 & 0\\ 0 & 0 & 0 & 0 & 0 & 0 & 0\\ 0 & 0 & -(1+\mu(\alpha^2+\beta^2))C_w & 0 & 0 & 0 & 0\\ 0 & 0 & 0 & 0 & 0 & 0 & 0\\ 0 & 0 & 0 & 0 & 0 & 0 & 0\\ 0 & 0 & 0 & 0 & 0 & 0 & 0\\ 0 & 0 & 0 & 0 & 0 & 0 & 0 \end{bmatrix} \tag{40}$$

$$\begin{aligned} &\kappa_{11} = A_{11}\alpha^2 + A_{66}\beta^2,\ \kappa_{12} = A_{12}\alpha\beta + A_{66}\alpha\beta,\ \kappa_{13} = 0,\\ &\kappa_{14} = B_{11}\alpha^2 + B_{66}\beta^2,\ \kappa_{15} = B_{12}\alpha\beta + B_{66}\alpha\beta,\\ &\kappa_{16} = D_{11}\alpha^2 + D_{66}\beta^2,\ \kappa_{17} = D_{12}\alpha\beta + D_{66}\alpha\beta,\\ &\kappa_{22} = A_{22}\beta^2 + A_{66}\alpha^2,\ \kappa_{23} = 0,\\ &\kappa_{24} = B_{12}\alpha\beta + B_{66}\alpha\beta,\ \kappa_{25} = B_{22}\beta^2 + B_{66}\alpha^2,\\ &\kappa_{26} = D_{12}\alpha\beta + D_{66}\alpha\beta,\ \kappa_{27} = D_{22}\beta^2 + D_{66}\alpha^2,\\ &\kappa_{33} = (A_{55}\alpha^2 + A_{44}\beta^2) - (1+\mu(\alpha^2+\beta^2))\mathrm{K}_w,\\ &\kappa_{34} = A_{55}\alpha,\ \kappa_{35} = A_{44}\beta,\ \kappa_{36} = 2B_{55}\alpha,\\ &\kappa_{37} = 2B_{44}\beta,\ \kappa_{44} = D_{11}\alpha^2 + D_{66}\beta^2 + A_{55},\\ &\kappa_{45} = D_{12}\alpha\beta + D_{66}\alpha\beta,\ \kappa_{46} = E_{11}\alpha^2 + E_{66}\beta^2 + 2B_{55},\\ &\kappa_{47} = E_{12}\alpha\beta + E_{66}\alpha\beta,\ \kappa_{55} = D_{22}\beta^2 + D_{66}\alpha^2 + A_{44},\\ &\kappa_{56} = E_{12}\alpha\beta + E_{66}\alpha\beta,\ \kappa_{57} = E_{22}\beta^2 + E_{66}\alpha^2 + 2B_{44},\\ &\kappa_{66} = F_{11}\alpha^2 + F_{66}\beta^2 + 4D_{55},\ \kappa_{67} = F_{12}\alpha\beta + F_{66}\alpha\beta,\\ &\kappa_{77} = F_{22}\beta^2 + F_{66}\alpha^2 + 4D_{44}. \end{aligned} \tag{41}$$

$$F_{ij} = \begin{Bmatrix} 0\\ 0\\ \frac{4m_p g}{L_x L_y}(1+\mu(\alpha^2+\beta^2))\sin(\alpha x_p)\sin(\beta y_p)\\ 0\\ 0\\ 0 \end{Bmatrix} \tag{42}$$

Using state space method, equations of motions could be re written as

$$\dot{\chi} = A\chi + BU \tag{43}$$

where χ is the state vector defined as

$$\begin{aligned} \chi_i = \{&U\ \ V\ \ W\ \ \Phi_1\ \ \Psi_1\ \ \Phi_2\ \ \Psi_2\\ &\dot{U}\ \ \dot{V}\ \ \dot{W}\ \ \dot{\Phi}_1\ \ \dot{\Psi}_1\ \ \dot{\Phi}_2\ \ \dot{\Psi}_2\}^T \end{aligned} \tag{44}$$

and A and B are the state and input matrices written as

$$\mathrm{A} = \begin{bmatrix} 0 & I\\ \lambda^{-1}\kappa & \lambda^{-1}\zeta \end{bmatrix} \tag{45}$$

$$B = \begin{Bmatrix} 0 & \lambda^{-1}F \end{Bmatrix} \tag{46}$$

in order to continue the process of solving the problem, fourth-order Runge-Kutta (RK4) method for the system of ODEs is used. RK4 method is a numerical solution which is used to solve the state space equations with fixed size time steps. This method describes the solving process as

$$\begin{cases} \dot{\chi}_i = f_i(t, \chi_j) \\ {}^{n+1}\chi_i = {}^{n}\chi_i + \sum_{p=1}^{4} c_p\ {}^{n}K_p \end{cases} \qquad i,j = 1...14 \tag{47}$$

in which ^{n} and $^{n+1}$ describes the steps that variables are presented and c_p and K_p are the RK4 coefficients and slopes defined as

$$\begin{cases} c_1 = \tau/6,\ {}^{n}K_{1i} = f_i({}^{n}t, {}^{n}\chi_j) \\ c_2 = \tau/3,\ {}^{n}K_{2i} = f_i\left({}^{n}t + \frac{\tau}{2}, {}^{n}\chi_j + \frac{\tau}{2}{}^{n}K_{1j}\right) \\ c_3 = \tau/3,\ {}^{n}K_{3i} = f_i\left({}^{n}t + \frac{\tau}{2}, {}^{n}\chi_j + \frac{\tau}{2}{}^{n}K_{2j}\right) \\ c_4 = \tau/6,\ {}^{n}K_{4i} = f_i({}^{n}t + \tau, {}^{n}\chi_j + \tau\,{}^{n}K_{3j}) \end{cases} \tag{48}$$

where K_1 is the increment slope at the beginning of the interval which is also known as Euler method's slope, K_2 and K_3 are the slopes at the midpoint and K_4 is the slope at the end of the interval. With respect to the formulation of this study, f_i is also defined as

$$f_i = A_{ij}\chi + B_{ij}u \qquad i,j = 1...14 \tag{49}$$

In this case the nanoparticle is assumed to move linearly on the FG nanoplate with a constant velocity, instance position of the moving mass according to the time domain could be written in non-dimensional form as a function of time as

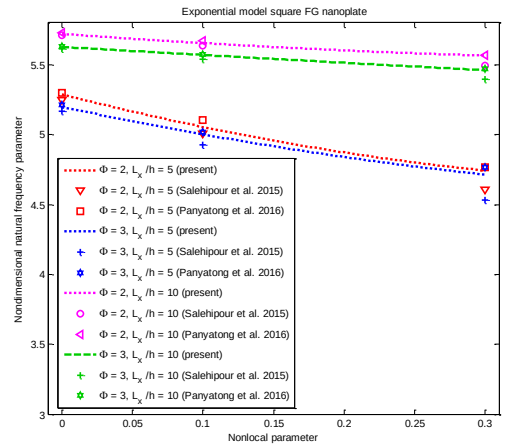

(a)

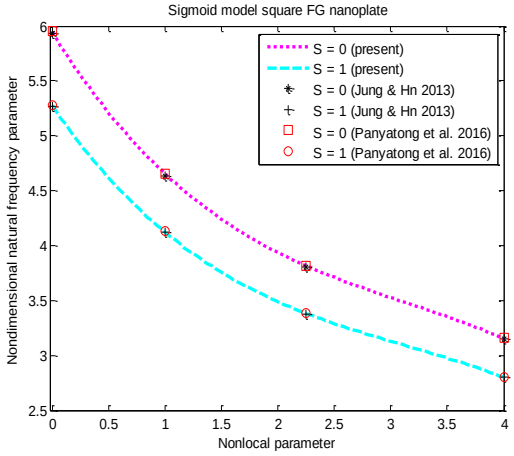

(b)

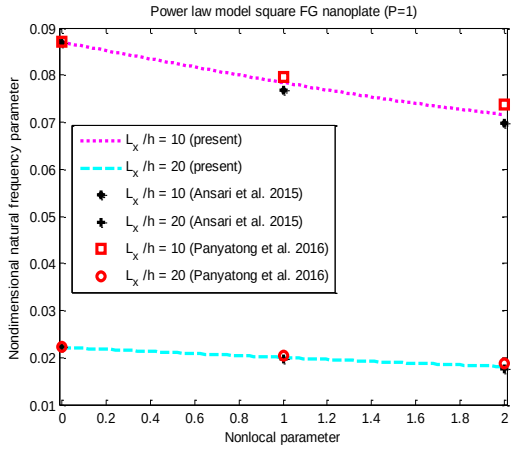

(c)

Fig. 2 Non-dimensional natural frequency parameter with respect to different nonlocal terms (a) Exponential FGM model (b) Sigmoid FGM model (c) Power-law FGM model

$$\begin{cases} x_p = \dfrac{V\cos(\theta)}{L_x}t \\ y_p = \dfrac{V\sin(\theta)}{L_y}t \end{cases} \tag{50}$$

Table 1 Non-dimensional maximum transverse deflection versus velocity of thin isotropic square plate

V	15.6	31.2	62.4	93.6	124.8	156	250
T	0.125	0.25	0.5	0.75	1	1.25	2
Present study	1.0357	1.1326	1.2614	1.5824	1.7075	1.7206	1.5487
Ghafoori and Asghari (2010)	1.048	1.33	1.275	1.573	1.702	1.714	1.539
Ghafoori and Asghari (2010)	1.063	1.412	1.291	1.643	1.743	1.737	1.556
Taheri and Ting (1989)	1.049	1.121	1.266	-	1.703	-	1.540
Taheri (1987)	1.042	1.082	1.266	-	1.662	-	1.518
Yoshida and Weaver (1971)	1.055	1.112	1.252	-	1.7	-	1.54
Filho (1966)	-	1.11	1.24	-	1.68	-	1.54
Kadivar and Mohebpour (1998)	1.052	1.133	1.265	1.571	1.692	1.717	1.535
Kadivar and Mohebpour (1998)	1.063	1.151	1.281	1.586	1.704	1.727	1.524
Kadivar and Mohebpour (1998)	1.063	1.151	1.281	1.585	1.704	1.727	1.542
Meirovitch (1967)	1.025	1.121	1.258	1.572	1.701	1.719	1.548
Esen (2013)	1.045	1.350	1.273	1.572	1.704	1.716	1.542

Table 2 Non-dimensional natural frequency parameter for sigmoid square FG nanoplate on elastic foundation

	$S = 0.5$				$S = 2$			
K	0	10	50	100	0	10	50	100
ω_{11}	0.30837	0.30946	0.31765	0.32632	0.27987	0.28136	0.28932	0.29921
Panyatong *et al.* (2016)	0.3086	0.3104	0.3178	0.3268	0.2806	0.2827	0.2907	0.3005
ω_{11}	0.61102	0.61338	0.61754	0.62245	0.56195	0.56298	0.56712	0.57215
Panyatong *et al.* (2016)	0.6139	0.6148	0.6184	0.6229	0.5624	0.5634	0.5673	0.5722
ω_{11}	0.81914	0.81845	0.82241	0.82483	0.75476	0.75246	0.75584	0.76193
Panyatong *et al.* (2016)	0.8193	0.8200	0.8227	0.8260	0.7549	0.7557	0.7585	0.7621

Table 3 Non-dimensional natural frequency parameter for exponential square FG nanoplate on elastic foundation

	$\emptyset = 0.1$				$\emptyset = 2$			
K	0	10	50	100	0	10	50	100
ω_{11}	0.17254	0.17691	0.18989	0.20047	0.19154	0.19578	0.20989	0.22516
Panyatong *et al.* (2016)	0.1753	0.1786	0.1909	0.2053	0.1937	0.1972	0.2107	0.2264
ω_{11}	0.34985	0.35012	0.35489	0.36542	0.38321	0.38489	0.39025	0.39978
Panyatong *et al.* (2016)	0.3515	0.3531	0.3594	0.3670	0.3845	0.3862	0.3930	0.4014
ω_{11}	0.47013	0.47058	0.47651	0.48089	0.50995	0.51123	0.51569	0.52357
Panyatong *et al.* (2016)	0.4714	0.4726	0.4772	0.4829	0.5122	0.5134	0.5185	0.5248

where V is the velocity of the nanoparticle and θ is the angle of the path with x axis.

4. Results and discussion

In this study, dynamic response of FG nanoplates resting on a viscoelastic medium carrying a moving nanoparticle is obtained for different paths and different type of FG materials. In order to verify the current methodology, different types of verifications are done. First, the plate is

Table 4 Non-dimensional natural frequency parameter for power law square FG nanoplate on elastic foundation

	$P=0.5$				$P=2$			
K	0	10	50	100	0	10	50	100
ω_{11}	0.32613	0.32097	0.33469	0.34267	0.26628	0.26912	0.27813	0.28786
Panyatong *et al.* (2016)	0.3282	0.3299	0.3365	0.3445	0.2671	0.2694	0.2783	0.2890
ω_{11}	0.65231	0.65321	0.65589	0.66054	0.52794	0.52874	0.53422	0.53947
Panyatong *et al.* (2016)	0.6547	0.6555	0.6587	0.6627	0.5305	0.5316	0.5360	0.5415
ω_{11}	0.87525	0.87565	0.87781	0.87994	0.70688	0.70798	0.71189	0.71584
Panyatong *et al.* (2016)	0.8752	0.8758	0.8782	0.8812	0.7081	0.7089	0.7121	0.7162

assumed to be at macro scale by neglecting the nonlocal terms. Material properties are also assumed to be isotropic by defining the same properties for the first and second materials of FG plate. Results are achieved for different velocities in different timelines and compared to those obtained in previous literatures which is presented in Table 1. Accordingly, it can be seen that results are in a good agreement with previous works on macro-scale problems.

Also, in order to verify the material variation modeling, natural frequency parameter which is defined in Panyatong *et al.* (2016) is calculated for different power law, sigmoid and exponential functionally graded plates and the results are compared to those presented in previous studies. Table 2 presents it for sigmoid functionally graded materials, table 3 denotes the frequency parameters for exponentially varying material properties for different exponential parameters and furthermore, table 4 presents it for power law FG materials for different power law indexes. Verification is also done for different nonlocal parameters and the results are compared to previous studies (Panyatong *et al.* 2016, Jung and Hn 2013, Salehipour *et al.* 2015, Ansari *et al.* 2015) and respectively presented in Fig. 2 which are in a great agreement.

After verifying the current formulation, to understand the effects of different material, motion and scale parameters, parametric study is presented. Material of the FG nanoplate is assumed to vary from aluminum (Al) to alumina (Al_2O_3), therefore for the power law and sigmoid varying materials, properties are defined as $E_{Al_2O_3}=380Gpa$, $E_{Al}=70Gpa$, $\rho_{Al_2O_3}=3.800\ kg/m^3$, $\rho_{Al_2O_3}=2.707\ kg/m^3$, $\vartheta=0.3$ and for exponential model of FG materials $E_{Al}=70Gpa$, $\rho_{Al}=2.702\ kg/m^3$, $\vartheta=0.3$. Other geometrical parameters are assumed to be $L_x=L_y=10\,nm$ for the lengths and $h=2\,nm$ for the thickness of nanoplate. Moreover, for the viscoelastic foundation, elastic and damping parameters are defined as $k=K_wL_x^4/A_{11}=100$ and $c=C_wL_x^4/A_{11}=10$. Deflection of FG nanoplate is presented in nondimensional form by dividing the deflection on the maximum static deflection of isotropic plate with a concentrated mass in middle of the plane which is written as

$$W_{st}=\frac{4mg}{\pi^2 DL_xL_y}\sum_{m=1}^{m_j}\sum_{n=1}^{n_i}\frac{\sin(\frac{m\pi}{2})\sin(\frac{n\pi}{2})\sin(\frac{m\pi}{L_x}x_1)\sin(\frac{n\pi}{L_y}x_2)}{\left[\left(\frac{m}{L_x}\right)^2+\left(\frac{n}{L_y}\right)^2\right]^2} \tag{51}$$

Table 5 Non-dimensional maximum transverse deflection versus nonlocal parameter for Power law FG nanoplate

		Maximum non-dimensional deformation parameter (W_{max}/W_{st})				
t	P	$\mu=0$	$\mu=0.1$	$\mu=0.3$	$\mu=0.5$	$\mu=0.7$
	0	0.024657	0.177861	0.476060	0.760532	1.032961
	0.5	0.037998	0.265769	0.701308	1.106671	1.486675
0.2 T	1	0.051570	0.34946	0.909142	1.418392	1.886109
	2	0.071090	0.469573	1.199588	1.844862	2.421887
	4	0.083751	0.566478	1.435325	2.189563	2.849409
	0	0.050232	0.190947	0.456798	0.704200	0.934398
	0.5	0.079768	0.295650	0.690914	1.044113	1.361192
0.4 T	1	0.111874	0.403557	0.919970	1.362943	1.747874
	2	0.157873	0.553947	1.223307	1.768592	2.223780
	4	0.180806	0.637949	1.393710	1.994534	2.485719
	0	0.051512	0.199493	0.485105	0.757659	1.018003
	0.5	0.081991	0.310268	0.741264	1.141038	1.513732
0.6 T	1	0.115311	0.425731	0.997634	1.512692	1.980989
	2	0.163365	0.589174	1.347467	2.005063	2.582980
	4	0.187366	0.682099	1.552197	2.296680	2.943007
	0	0.026392	0.184779	0.499413	0.806146	1.104959
	0.5	0.040970	0.278145	0.745878	1.195459	1.626571
0.8 T	1	0.056092	0.369212	0.980685	1.560388	2.107224
	2	0.078149	0.501766	1.316932	2.071827	2.766875
	4	0.092102	0.605736	1.581338	2.467668	3.267397
	0	0.000001	0.000029	0.000393	0.001522	0.003750
	0.5	0.000004	0.000112	0.001372	0.005066	0.011879
T	1	0.000013	0.000305	0.003311	0.011404	0.025615
	2	0.000038	0.000823	0.008012	0.025860	0.055462
	4	0.000056	0.001187	0.012131	0.039542	0.084703

Accordingly, the number of terms in the series expansions in Eq. (36), Eq. (37) and Eq. (51) is chosen as $n_i=m_j=30$ in which convergence of the results are seen.

4.1 Influence of the material variation on the dynamic deformation

As mentioned before, three types of material variation for FG model are proposed and formulated. In this section, for all three kinds of FGM, effect of material variation on the maximum dynamic deflection of nanoplate is calculated for different nonlocal parameters. Dynamic deflection is proposed in non-dimensional form by diving it on the maximum static deflections of isotropic aluminum thin plate under a static load in the middle. In Table 5, this influence is obtained for power law FG nanoplate with different power law index and nonlocal parameter. Viscoelastic foundation is used and the stiffness and damping parameters are defined as $k=100$ and $c=10$.

Accordingly, it can be seen that for all the power index parameters, increasing the nonlocal parameter leads to a higher maximum deflection in FG nanoplates and

Table 6 Non-dimensional maximum transverse deflection versus nonlocal parameter for Sigmoid FG nanoplate

		Maximum non-dimensional deformation parameter (W_{max}/W_{st})				
t	S	$\mu = 0$	$\mu = 0.1$	$\mu = 0.3$	$\mu = 0.5$	$\mu = 0.7$
	0	0.041394	0.296976	0.782790	1.233655	1.652889
	0.5	0.045622	0.319400	0.837191	1.313680	1.754463
0.2 T	1	0.051569	0.349462	0.909155	1.418398	1.886111
	2	0.061392	0.395034	1.015218	1.571140	2.074946
	4	0.072336	0.441156	1.117954	1.715986	2.252147
	0	0.084183	0.316233	0.739168	1.114708	1.449708
	0.5	0.095444	0.352305	0.815000	1.220019	1.577161
0.4 T	1	0.111874	0.403559	0.919979	1.362920	1.747889
	2	0.140128	0.488181	1.086286	1.582990	2.004020
	4	0.173157	0.582088	1.260955	1.805748	2.255031
	0	0.086534	0.332633	0.796440	1.225699	1.625947
	0.5	0.098219	0.370942	0.880286	1.346506	1.776645
0.6 T	1	0.115311	0.425733	0.997655	1.512692	1.980976
	2	0.144822	0.517078	1.186752	1.773420	2.294027
	4	0.179527	0.619982	1.390315	2.043666	2.608956
	0	0.044539	0.310575	0.832222	1.330955	1.806409
	0.5	0.049295	0.335232	0.895507	1.428992	1.935476
0.8 T	1	0.056092	0.369212	0.980734	1.560314	2.107223
	2	0.067500	0.422133	1.111760	1.759508	2.364574
	4	0.080617	0.477072	1.246059	1.960046	2.619564
	0	0.000005	0.000156	0.001743	0.006458	0.015299
	0.5	0.000008	0.000187	0.002297	0.008283	0.019221
T	1	0.000013	0.000305	0.003308	0.011403	0.025623
	2	0.000028	0.000603	0.005672	0.017928	0.038236
	4	0.000054	0.001138	0.009636	0.027470	0.055110

Table 7 Non-dimensional maximum transverse deflection versus nonlocal parameter for Exponential varying material properties in FG nanoplate

		Maximum non-dimensional deformation parameter (W_{max}/W_{st})				
t	Φ	$\mu = 0$	$\mu = 0.1$	$\mu = 0.3$	$\mu = 0.5$	$\mu = 0.7$
	0.1	0.128982	0.901107	2.211706	3.265513	4.124142
	0.5	0.129024	0.901235	2.211870	3.265777	4.124508
0.2 T	1	0.129157	0.901728	2.212691	3.266712	4.125568
	2	0.129689	0.903463	2.215830	3.270482	4.129608
	4	0.131901	0.910565	2.228317	3.285519	4.145600
	0.1	0.259692	0.920468	1.936144	2.681779	3.255042
	0.5	0.259838	0.920849	1.936678	2.682495	3.255768
0.4 T	1	0.260295	0.921998	1.938598	2.684681	3.258073
	2	0.262138	0.926689	1.946150	2.693413	3.267234
	4	0.269747	0.945892	1.976936	2.728776	3.304343
	0.1	0.270340	0.998915	2.227365	3.228776	4.072776
	0.5	0.270495	0.999364	2.228083	3.229594	4.073733
0.6 T	1	0.270980	1.000661	2.230343	3.232263	4.076492
	2	0.272941	1.005871	2.239306	3.242880	4.087768
	4	0.281069	1.027459	2.276035	3.286033	4.133276
	0.1	0.142517	0.972289	2.472169	3.741163	4.806577
	0.5	0.142571	0.972510	2.472620	3.741707	4.807284
0.8 T	1	0.142741	0.973059	2.473898	3.743519	4.809322
	2	0.143424	0.975488	2.479296	3.750700	4.817689
	4	0.146224	0.985281	2.500651	3.779786	4.851237
	0.1	0.000158	0.003330	0.037961	0.120313	0.245702
	0.5	0.000157	0.003323	0.037981	0.120392	0.245791
T	1	0.000159	0.003326	0.038080	0.120574	0.246110
	2	0.000164	0.003364	0.038413	0.121323	0.247319
	4	0.000179	0.003625	0.039752	0.124456	0.252305

moreover, it is obtained that increasing the power law parameter (P) increases the deflection in FG nanoplate in all timelines for all nonlocal parameters.

Such behavior was expected from these kind of FG materials because as shown in Table 4 and Fig 2(c), increasing the power law parameter caused a reduction in natural frequency parameter which means the plate shows more flexibility in different loading situations. These deflection parameters are presented in different timelines from the beginning of the movement until the nanoparticle leaves the system. For sigmoid varying material properties, same analysis has been done. As well as the power law FG nanoplates, sigmoid varying results are obtained in Table 6. Like before increasing the sigmoid varying parameter (S) increases the maximum deflection parameter which was also predicted due to the behavior of natural frequency parameter in Fig. 2(b) and Table 2. Also, increasing the nonlocal parameter causes a higher deflection in sigmoid varying FG nanoplates. Results are fully presented in Table 6 for different timelines, sigmoid and nonlocal parameters. Likewise, same analysis has been done for exponentially varying properties and results are presented in Table 7.

4.2 Influence of the viscoelastic foundation on the dynamic behavior

In this study, it is assumed that FG nanoplate is resting on a viscoelastic medium which is modeled after Kelvin-Voigt theory. In order to understand the effects of this foundation on decreasing the deflection in the plate and avoiding the resonance, different amounts are assumed for both stiffness and damping parameters of foundation. As shown in Fig. 3(a), by having constant amount for different geometrical and natural properties of exponential FGM nanoplate, effects of stiffness parameters are obtained for different nonlocal parameters. In the same way, these effects on maximum non-dimensional dynamic deformation of sigmoid and power law FGM modeled nanoplates are obtained in Fig. 3(b) and Fig. 3(c). It can be seen that increasing the coupling parameter will decrease the deflections and it has its most effect for higher nonlocal parameters for all three FG nanoplate models. Damping parameter is also studied for all three FG nanoplate models and the effects are presented in Fig. 4. Increasing the damping parameter also leads to lower deformations.

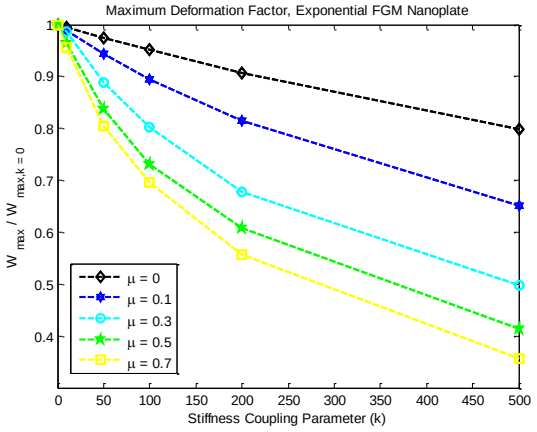

(a)

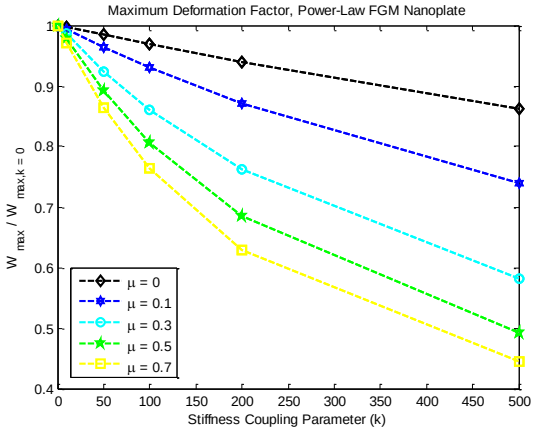

(b)

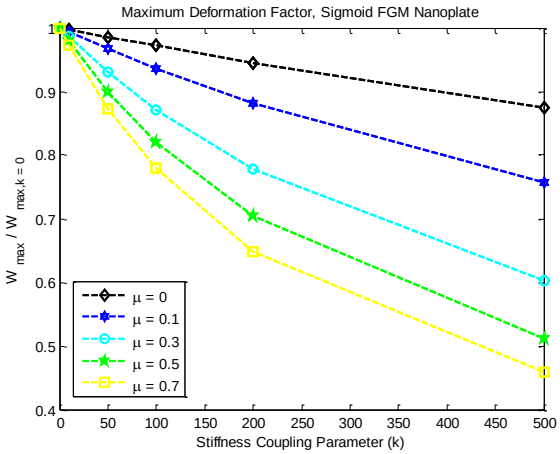

(c)

Fig. 3 Maximum non-dimensional forced deformation with respect to stiffness coupling term 'k' for different nonlocal parameters (a) Exponential FGM model (b) Sigmoid FGM model (c) Power-law FGM model

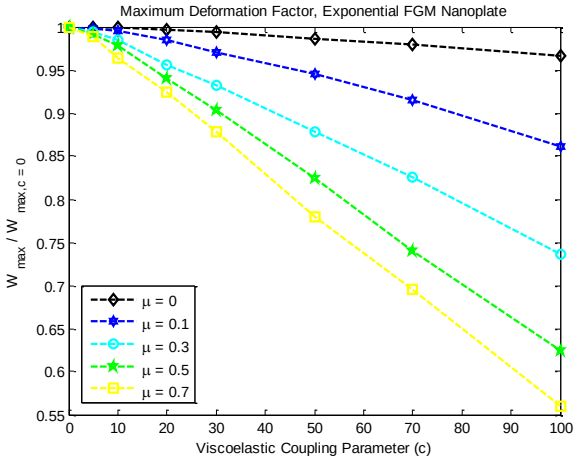

(a)

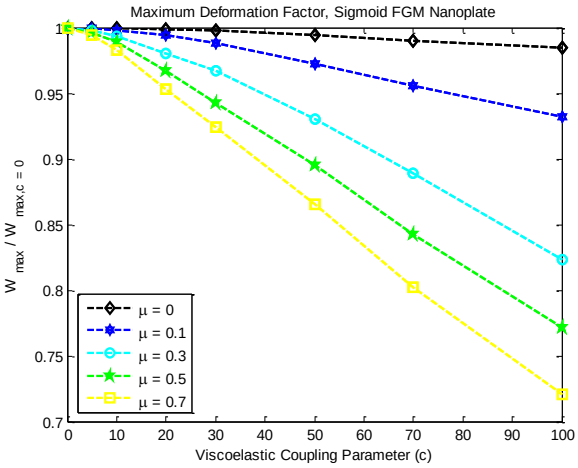

(b)

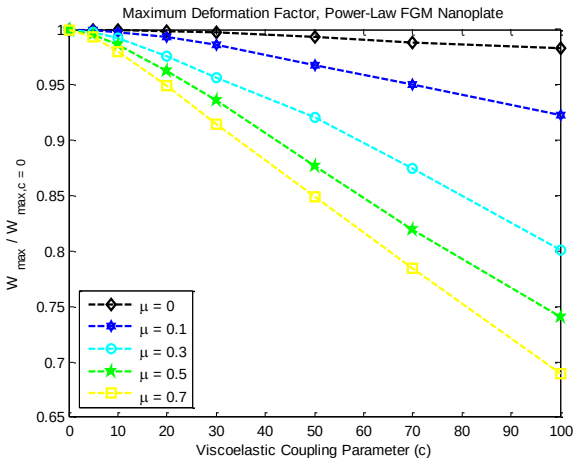

(c)

Fig. 4 Maximum non-dimensional forced deformation with respect to viscoelastic coupling term '*c*' for different nonlocal parameters (a) Exponential FGM model (b) Sigmoid FGM model (c) Power-law FGM model

Deformation parameter shows more sensitivity to damping variation compared to stiffness parameter.

4.3 Influence of the velocity parameter on the dynamic behavior

The velocity of the moving nanoparticle is one of the most important parameters effecting the deflection in nanoplate. Different velocity parameters are assumed for moving nanoparticle while other parameters remained constant. Fig. 5 shows these effects on non-dimensional

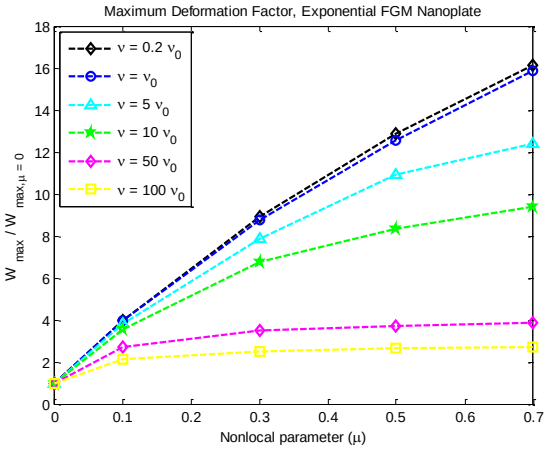

(a)

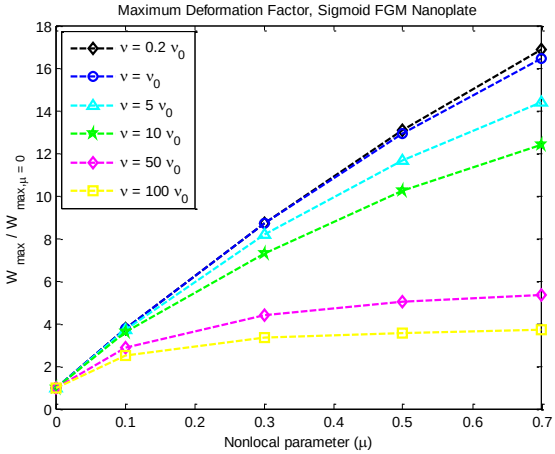

(b)

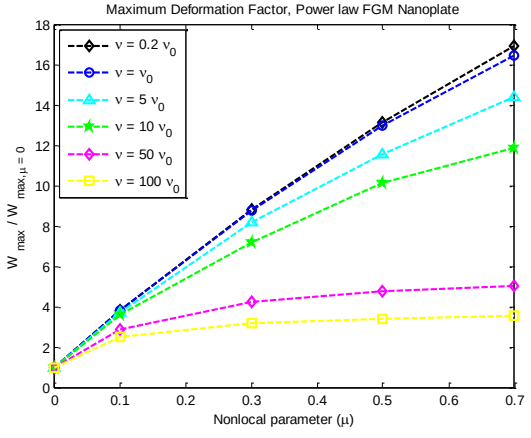

(c)

Fig. 5 Maximum non-dimensional forced deformation with respect to velocity of nanoparticle for different nonlocal parameters (a) Exponential FGM model (b) Sigmoid FGM model (c) Power-law FGM model

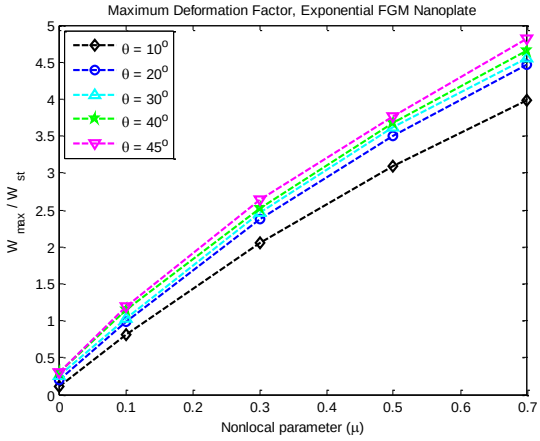

(a)

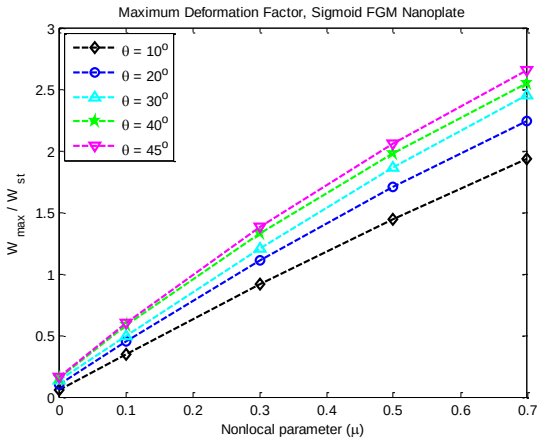

(b)

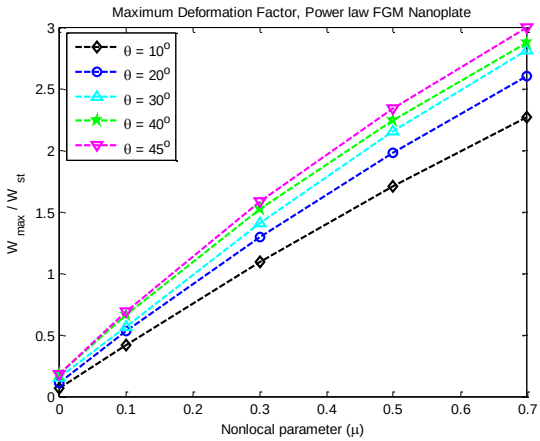

(c)

Fig. 6 Maximum non-dimensional forced deformation parameter with respect to the angle of nanoparticles path for different nonlocal parameters (a) Exponential FGM model (b) Sigmoid FGM model (c) Power-law FGM model

maximum deflection for power law, sigmoid and exponential FG models of nanoplate while nanoparticle passes through. It can be seen that increasing the velocity parameter decreases the deformation in all models. Deflection term is shown in a non-dimensional form by dividing the results to the deflection without small scale effects ($\mu = 0$) and it shows its most sensitivity to velocity variation from $5v_0$ to $50v_0$ and for higher velocity terms, deflections merge to a specific amount.

4.4 Influence of the angle on the dynamic behavior

In order to obtain the influence of the path of the

moving nanoparticle, the angle between the velocity vector and the x axis is varied from 0 to 45 degrees and deflections are achieved for different nonlocal parameter. By having the same geometrical and natural properties as before, dynamic deflection parameter is presented for FGM models in Fig. 6.

5. Conclusions

This paper presents three-dimensional dynamic behavior of functionally graded nanoplates carrying a moving nanoparticle/load. Second order shear deformation and Eringen's nonlocal theory are used to model the nanoplate. Material variation is assumed to be through the thickness using power law, sigmoid and exponential variation functions. Moreover, nanoplate is assumed to be resting on a viscoelastic medium which is modeled using Kelvin-Voigt theory and nanoparticle is modeled as a concentrated mass which passes through an arbitrary linear path. Equations of motion are presented and solved using the Galerkin, state space and fourth-order Runge-Kutta methods and the schematic behavior of FG nanoplate in all the three cases are presented. In order to clarify the effects of different parameters, a comprehensive parametric study is done by analyzing material variation methods, nonlocal effects, stiffness and damping effects in viscoelastic foundation, velocity and the moving path of nanoparticle and its effects on dynamic behavior of FG nanoplate. It is shown that adding material variation and nonlocal effects changes the behavior of nanoplate and have a significant effect on the dynamic deflections under a moving nanoparticle.

Acknowledgments

This research received no specific grant from any funding agency in the public.

References

Abualnour, M., Houari, M.S.A., Tounsi, A. and Mahmoud, S.R. (2018), "A novel quasi-3D trigonometric plate theory for free vibration analysis of advanced composite plates", *Compos. Struct.*, **184**, 688-697.

Ahouel, M., Houari, M.S.A., Bedia, E.A. and Tounsi, A. (2016), "Size-dependent mechanical behavior of functionally graded trigonometric shear deformable nanobeams including neutral surface position concept", *Steel Compos. Struct.*, **20**(5), 963-981.

Akbas, S.D. (2017), "Post-buckling responses of functionally graded beams with porosities", *Steel Compos. Struct.*, **24**(5), 579-589.

Ansari, R., Shojaei, M.F., Shahabodini, A. and Bazdid-Vahdati, M. (2015), "Three-dimensional bending and vibration analysis of functionally graded nanoplates by a novel differential quadrature-based approach", *Compos. Struct.*, **131**, 753-764.

Arani, G.A., Haghparast, E. and Zarei, H.B. (2017), "Vibration analysis of functionally graded nanocomposite plate moving in two directions", *Steel Compos. Struct.*, **23**(5), 529-541.

Arani, A.G., Kolahchi, R. and Afshar, H.G. (2015), "Dynamic analysis of embedded PVDF nanoplate subjected to a moving nanoparticle on an arbitrary elliptical path", *J. Brazil. Soc. Mech. Sci. Eng.*, **37**(3), 973-986.

Arefi, M. (2014), "Elastic solution of a curved beam made of functionally graded materials with different cross sections", *Steel Compos. Struct.*, **18**(3), 659-672.

Asghari, M., Ahmadian, M.T., Kahrobaiyan, M.H. and Rahaeifard, M. (2017), "On the size-dependent behavior of functionally graded micro-beams with porosities", *Struct. Eng. Mech.*, **64**(5), 527-541.

Barati, M.R., Zenkour, A.M. and Shahverdi, H. (2016), "Thermo-mechanical buckling analysis of embedded nanosize FG plates in thermal environments via an inverse cotangential theory", *Compos. Struct.*, **141**, 203-212.

Belabed, Z., Houari, M.S.A., Tounsi, A., Mahmoud, S.R. and Bég, O.A. (2014), "An efficient and simple higher order shear and normal deformation theory for functionally graded material (FGM) plates", *Compos.*: *Part B*, **60**, 274-283.

Beldjelili, Y., Tounsi, A. and Mahmoud, S.R. (2016), "Hygro-thermo-mechanical bending of S-FGM plates resting on variable elastic foundations using a four-variable trigonometric plate theory", *Smart Struct. Syst.*, **18**(4), 755-786.

Bellifa, H., Benrahou, K.H., Hadji, L., Houari, M.S.A. and Tounsi, A. (2016), "Bending and free vibration analysis of functionally graded plates using a simple shear deformation theory and the concept the neutral surface position", *J. Brazil. Soc. Mech. Sci. Eng.*, **38**(1), 265-275.

Belkorissat, I., Houari, M.S.A., Tounsi, A., Bedia, E.A. and Mahmoud, S.R. (2015), "On vibration properties of functionally graded nano-plate using a new nonlocal refined four variable model", *Steel Compos. Struct.*, **18**(4), 1063-1081.

Bennoun, M., Houari, M.S.A. and Tounsi, A. (2016), "A novel five variable refined plate theory for vibration analysis of functionally graded sandwich plates", *Mech. Adv. Mater. Struct.*, **23**(4), 423-431.

Besseghier, A., Houari, M.S.A., Tounsi, A. and Mahmoud, S.R. (2017), "Free vibration analysis of embedded nanosize FG plates using a new nonlocal trigonometric shear deformation theory", *Smart Struct. Syst.*, **19**(6), 601-614.

Bouafia, K., Kaci, A., Houari, M.S.A., Benzair, A. and Tounsi, A. (2017), "A nonlocal quasi-3D theory for bending and free flexural vibration behaviors of functionally graded nanobeams", *Smart Struct. Syst.*, **19**(2), 115-126.

Bouderba, B., Houari, M.S.A. and Tounsi, A. (2013), "Thermomechanical bending response of FGM thick plates resting on Winkler-Pasternak elastic foundations", *Steel Compos. Struct.*, **14**(1), 85-104.

Bouderba, B., Houari, M.S.A., Tounsi, A. and Mahmoud, S.R. (2016), "Thermal stability of functionally graded sandwich plates using a simple shear deformation theory", *Struct. Eng. Mech.*, **58**(3), 397-422.

Bourada, M., Kaci, A., Houari, M.S.A. and Tounsi, A. (2015), "A new simple shear and normal deformations theory for functionally graded beams", *Steel Compos. Struct.*, **18**(2), 409-423.

Bousahla, A.A., Benyoucef, S., Tounsi, A. and Mahmoud, S.R. (2016), "On thermal stability of plates with functionally graded coefficient of thermal expansion", *Struct. Eng. Mech.*, **60**(2), 313-335.

Bounouara, F., Benrahou, K.H. Belkorissat, I. and Tounsi, A. (2016), "A nonlocal zeroth-order shear deformation theory for free vibration of functionally graded nanoscale plates resting on elastic foundation", *Steel Compos. Struct.*, **20**(2), 227-249.

Chaht, L., Kaci, A., Houari, M.S.A., Tounsi, A., Anwar Bég, O., and Mahmoud, M. (2015), "Bending and buckling analyses of functionally graded material (FGM) size-dependent nanoscale beams including the thickness stretching effect", *Steel Compos. Struct.*, **18**(2), 425-442.

Chikh, A., Tounsi, A., Hebali, H. and Mahmoud, S.R. (2017), "Thermal buckling analysis of cross-ply laminated plates using a simplified HSDT", *Smart Struct. Syst.*, **19**(3), 289-297.

Draiche, K., Tounsi, A. and Mahmoud, S.R. (2016), "A refined theory with stretching effect for the flexure analysis of laminated composite plates", *Geomech. Eng.*, **5**(11), 671-690.

El-Wazery, M.S. and El-Desouky, A.R. (2015), "A review on functionally graded ceramic-metal materials", *J. Mater. Environ. Sci.*, **6**(5), 1369-1376.

Eringen, A.C. (2002), *Nonlocal Continuum Field Theories*, Springer Science & Business Media.

Esen, I. (2013), "A new finite element for transverse vibration of rectangular thin plates under a moving mass", *Fin. Elem. Analy. Des.*, **66**, 26-35.

Fahsi, A., Tounsi, A., Hebali, H., Chikh, A., Adda Bedia, E.A. and Mahmoud, S.R. (2017), "A four variable refined nth-order shear deformation theory for mechanical and thermal buckling analysis of functionally graded plates", *Geomech. Eng.*, **13**(3), 385-410.

Ghafoori, E. and Asghari, M. (2010), "Dynamic analysis of laminated composite plates traversed by a moving mass based on a first-order theory", *Compos. Struct.*, **92**(8), 1865-1876.

Hamidi, A., Houari, M.S.A., Mahmoud, S.R. and Tounsi, A. (2015), "A sinusoidal plate theory with 5-unknowns and stretching effect for thermomechanical bending of functionally graded sandwich plates", *Steel Compos. Struct.*, **18**(1), 235-253.

Hashemi, S.H. and Khaniki, H.B. (2016a), "Free vibration analysis of functionally graded materials non-uniform beams", *Int. J. Eng.-Trans. C: Asp.*, **29**(12), 1734.

Hashemi, S.H. and Khaniki, H.B. (2016b), "Analytical solution for free vibration of a variable cross-section nonlocal nanobeam", *Int. J. Eng.-Trans. B: Appl.*, **29**(5), 688-696.

Hashemi, S.H. and Khaniki, H.B. (2017a), "Dynamic behavior of multi-layered viscoelastic nanobeam system embedded in a viscoelastic medium with a moving nanoparticle", *J. Mech.*, **33**(5), 559-575.

Hashemi, S.H. and Khaniki, H.B. (2017b), "Dynamic response of multiple nanobeam system under a moving nanoparticle", *Alexandr. Eng. J.*

Hebali, H., Tounsi, A., Houari, M.S.A., Bessaim, A. and Bedia, E.A.A. (2014), "A new quasi-3D hyperbolic shear deformation theory for the static and free vibration analysis of functionally graded plates", *ASCE J. Eng. Mech.*, **140**, 374-383.

Hebali, H., Bakora, A., Tounsi, A. and Kaci, A. (2017), "A novel four variable refined plate theory for bending, buckling, and vibration of functionally graded plates", *Steel Compos. Struct.*, **23**(3), 473-495.

Hosseini Hashemi, S. and Bakhshi Khaniki, H. (2017), "Vibration analysis of a Timoshenko non-uniform nanobeam based on nonlocal theory: An analytical solution", *Int. J. Nano Dimens.*, **8**(1), 70-81.

Houari, M.S.A., Tounsi, A., Bessaim, A. and Mahmoud, S.R. (2016), "A novel four variable refined plate theory for bending, buckling, and vibration of functionally graded plates", *Steel Compos. Struct.*, **22**(2), 257-276.

Jung, W.Y. and Hn, S.C. (2013), "Analysis of sigmoid functionally graded material (S-FGM) nanoscale plates using the nonlocal elasticity theory", *Math. Probl. Eng.*, 1-10.

Kadivar, M.H. and Mohebpour, S.R. (1998), "Finite element dynamic analysis of unsymmetric composite laminated beams with shear effect and rotary inertia under the action of moving loads", *Fin. Elem. Analy. Des.*, **29**(3), 259-273.

Khaniki, H.B. (2018), "On vibrations of nanobeam systems", *Int. J. Eng. Sci.*, **124**, 85-103.

Khaniki, H.B. and Hashemi, S.H. (2017a), "Free vibration analysis of nonuniform microbeams based on modified couple stress theory: An analytical solution", *Int. J. Eng.-Trans. B: Appl.*, **30**(2), 311-320.

Khaniki, H.B. and Hosseini-Hashemi, S. (2017b), "Buckling analysis of tapered nanobeams using nonlocal strain gradient theory and generalized differential quadrature method", *Mater. Res. Expr.*, **4**(6), 065003.

Khaniki, H.B. and Hosseini-Hashemi, S. (2017c), "Dynamic transverse vibration characteristics of nonuniform nonlocal strain gradient beams using the generalized differential quadrature method", *Eur. Phys. J. Plus*, **132**(11), 500.

Khaniki, H.B. and Hosseini-Hashemi, S. (2017d), "The size-dependent analysis of multilayered microbridge systems under a moving load/mass based on the modified couple stress theory", *Eur. Phys. J. Plus*, **132**(5), 1-18.

Khaniki, H.B. and Hosseini-Hashemi, S. (2017e), "Dynamic response of biaxially loaded double-layer viscoelastic orthotropic nanoplate system under a moving nanoparticle", *Int. J. Eng. Sci.*, **115**, 51-72.

Khaniki, H.B., Hosseini-Hashemi, S. and Nezamabadi, A. (2017), "Buckling analysis of nonuniform nonlocal strain gradient beams using generalized differential quadrature method", *Alexandr. Eng. J.*

Khetir, H., Bouiadjra, M.B., Houari, M.S.A., Tounsi, A. and Mahmoud, S.R. (2017), "A new nonlocal trigonometric shear deformation theory for thermal buckling analysis of embedded nanosize FG plates", *Struct. Eng. Mech.*, **64**(4), 391-402.

Kiani, K. (2011a), "Small-scale effect on the vibration of thin nanoplates subjected to a moving nanoparticle via nonlocal continuum theory", *J. Sound Vibr.*, **330**(20), 4896-4914.

Kiani, K. (2011b), "Nonlocal continuum-based modeling of a nanoplate subjected to a moving nanoparticle. Part I: Theoretical formulations", *Phys. E: Low-Dimens. Syst. Nanostruct.*, **44**(1), 229-248.

Kiani, K. (2013), "Vibrations of biaxially tensioned-embedded nanoplates for nanoparticle delivery", *Ind. J. Sci. Technol.*, **6**(7), 4894-4902.

Lomakin, V.A. (1966), "On the theory of deformation of micro-inhomogeneous bodies and its relation with the couple stress theory of elasticity", *J. Appl. Math. Mech.*, **30**(5), 1035-1042.

Mahi, A. and Tounsi, A. (2015), "A new hyperbolic shear deformation theory for bending and free vibration analysis of isotropic, functionally graded, sandwich and laminated composite plates", *Appl. Math. Model.*, **39**(9), 2489-2508.

Mahmoud, S.R. and Tounsi, A. (2017), "A new shear deformation plate theory with stretching effect for buckling analysis of functionally graded sandwich plates", *Steel Compos. Struct.*, **24**(5), 569-578.

Meftah, A., Bakora, A., Zaoui, F.Z., Tounsi, A. and El Abbes, A.B. (2017), "A non-polynomial four variable refined plate theory for free vibration of functionally graded thick rectangular plates on elastic foundation", *Steel Compos. Struct.*, **23**(3), 317-330.

Meirovitch, L. (1967), *Analytical Methods in Vibrations*, Macmillan, New York, U.S.A.

Menasria, A., Bouhadra, A., Tounsi, A., Bousahla, A.A. and Mahmoud, S.R. (2017), "A new and simple HSDT for thermal stability analysis of FG sandwich plates", *Steel Compos. Struct.*, **25**(2), 157-175.

Meziane, M.A.A., Abdelaziz, H.H. and Tounsi, A. (2014), "An efficient and simple refined theory for buckling and free vibration of exponentially graded sandwich plates under various boundary conditions", *J. Sandw. Struct. Mater.*, **16**(3), 293-318.

Mindlin, R.D. and Eshel, N.N. (1968), "On first strain-gradient theories in linear elasticity", *Int. J. Sol. Struct.*, **4**(1), 109-124.

Moradi-Dastjerdi, R. and Momeni, H. (2016), "Dynamic analysis of functionally graded nanocomposite plates reinforced by wavy carbon nanotube", *Steel Compos. Struct.*, **22**(2), 277-299.

Mouffoki, A., Adda Bedia, E.A., Houari, A., Tounsi, A. and Mahmoud, S.R. (2017), "Vibration analysis of nonlocal

advanced nanobeams in hygro-thermal environment using a new two-unknown trigonometric shear deformation beam theory", *Smart Struct. Syst.*, **20**(3), 369-383.
Nami, M.R. and Janghorban, M. (2015), "Dynamic analysis of isotropic nanoplates subjected to moving load using state-space method based on nonlocal second order plate theory", *J. Mech. Sci. Technol.*, **29**(6), 2423-2426.
Nguyen, H.X., Nguyen, T.N., Abdel-Wahab, M., Bordas, S.P.A., Nguyen-Xuan, H. and Vo, T.P. (2017), "A refined quasi-3D isogeometric analysis for functionally graded microplates based on the modified couple stress theory", *Comput. Meth. Appl. Mech. Eng.*, **313**, 904-940.
Panyatong, M., Chinnaboon, B. and Chucheepsakul, S. (2016), "Free vibration analysis of FG nanoplates embedded in elastic medium based on second-order shear deformation plate theory and nonlocal elasticity", *Compos. Struct.*, **153**, 428-441.
Rajasekaran, S. and Khaniki, H.B. (2017), "Bending, buckling and vibration of small-scale tapered beams", *Int. J. Eng. Sci.*, **120**, 172-188.
Saidi, H., Tounsi, A. and Bousahla, A.A. (2016), "A simple hyperbolic shear deformation theory for vibration analysis of thick functionally graded rectangular plates resting on elastic foundations", *Geomech. Eng.*, **11**(2), 289-307.
Salehipour, H., Shahidi, A.R. and Nahvi, H. (2015), "Modified nonlocal elasticity theory for functionally graded materials", *Int. J. Eng. Sci.*, **90**, 44-57.
Sallai, B., Hadji, L., Daouadji, T.H. and Adda Bedia, E.A. (2015), "Analytical solution for bending analysis of functionally graded beam", *Steel Compos. Struct.*, **19**(4), 829-841.
Shahsavari, D., Karami, B., Janghorban, M. and Li, L. (2017), "Dynamic characteristics of viscoelastic nanoplates under moving load embedded within visco-Pasternak substrate and hygrothermal environment", *Mater. Res. Expr.*, **4**(8), 085013.
Shahsavari, D. and Janghorban, M. (2017), "Bending and shearing responses for dynamic analysis of single-layer graphene sheets under moving load", *J. Brazil. Soc. Mech. Sci. Eng.*, 1-13.
Sola, A., Bellucci, D. and Cannillo, V. (2016), "Functionally graded materials for orthopedic applications-an update on design and manufacturing", *Biotechnol. Adv.*, **34**(5), 504-531.
Taheri, M.R. and Ting, E.C. (1989), "Dynamic response of plate to moving loads: Structural impedance method", *Comput. Struct.*, **33**(6), 1379-1393.
Taheri, M.R. (1987), "Dynamic response of plates to moving loads, structural impedance and finite element methods", Ph.D. Dissertation, Purdue University, U.S.A.
Tahouneh, V. (2017), "Using modified Halpin-Tsai approach for vibrational analysis of thick functionally graded multi-walled carbon nanotube plates", *Steel Compos. Struct.*, **23**(6), 657-668.
Talha, M. and Singh, B.N. (2010), "Static response and free vibration analysis of FGM plates using higher order shear deformation theory", *Appl. Math. Model.*, **34**(12), 3991-4011.
Tounsi, A., Houari, M.S.A. and Benyoucef, S. (2013), "A refined trigonometric shear deformation theory for thermoelastic bending of functionally graded sandwich plates", *Aerosp. Sci. Technol.*, **24**(1), 209-220.
Yoshida, D.M. and Weaver, W. (1971), "Finite element analysis of beams and plates with moving loads", *Publ. Int. Assoc. Brid. Struct. Eng.*, **31**(1), 179-195.
Uysal, M.U. (2016), "Buckling behaviours of functionally graded polymeric thin-walled hemispherical shells", *Steel Compos. Struct.*, **21**(4), 849-862.
Venancio-Filho, F. (1966), "Dynamic influence lines of beams and frames", *ASCE J. Struct. Div.*, **92**, 371-385.
Xiong, Q.L. and Tian, X. (2017), "Transient thermo-piezo-elastic responses of a functionally graded piezoelectric plate under thermal shock", *Steel Compos. Struct.*, **25**(2), 187-196.
Yahia, S.A., Atmane, H.A., Houari, M.S.A. and Tounsi, A. (2015), "Wave propagation in functionally graded plates with porosities using various higher-order shear deformation plate theories", *Struct. Eng. Mech.*, **53**(6), 1143-1165.
Zemri, A., Houari, M.S.A., Bousahla, A.A. and Tounsi, A. (2015), "A mechanical response of functionally graded nanoscale beam: An assessment of a refined nonlocal shear deformation theory beam theory", *Struct. Eng. Mech.*, **54**(4), 693-710.
Zidi, M., Tounsi, A., Houari, M.S.A. and Bég, O.A. (2014), "Bending analysis of FGM plates under hygro-thermo-mechanical loading using a four variable refined plate theory", *Aerosp. Sci. Technol.*, **34** 24-34.

CC